



Evaluation of Nontoxic Polymer Coatings with Potential Biofoul Release Properties Using EIS

E. Kus,^{a,*} M. A. Grunlan,^b W. P. Weber,^b and F. Mansfeld^{a,**,z}

^aCorrosion and Environmental Effects Laboratory, Department of Materials Science and Engineering, University of Southern California, Los Angeles, California 90089-0241, USA

^bDepartment of Chemistry, University of Southern California, Los Angeles, California 90089-1661, USA

The corrosion resistance of steel panels coated with pentasiloxanes has been evaluated by electrochemical impedance spectroscopy (EIS) during exposure to 0.5 N NaCl. Two fluorinated and a nonfluorinated pentasiloxane have been prepared to develop nontoxic polymer coatings with improved biofoul release properties. Depending on the terminal epoxy group type, two different cross-linking/cure chemistries were utilized. The first type of cross-linking reaction involved room-temperature UV cure with a photoacid catalyst and the second cross-linking reaction was phenol-catalyzed thermal cross-linking with α, ω -diaminoalkanes [$\text{NH}_2\text{-(CH}_2\text{)}_n\text{-NH}_2$]. The EIS data suggest that the nonfluorinated pentasiloxane provided better corrosion protection than the two fluorinated pentasiloxanes and that room-temperature UV cure with a photoacid catalyst provides better corrosion protection than phenol-catalyzed thermal cross-linking.

© 2005 The Electrochemical Society. [DOI: 10.1149/1.1923727] All rights reserved.

Manuscript submitted October 18, 2004; revised manuscript received January 18, 2005. Available electronically June 3, 2005.

On a ship's hull biofouling, which is the attachment of marine organisms on marine vessels and structures, leads to an increase in the hydrodynamic drag and therefore to increased power requirements and/or reduced speed. Presently used ablative coatings that contain biocides such as cupric oxide or organo-tin compounds are nonselective and considered to have a negative environmental impact.

The aim of this project is to develop nontoxic, environmentally friendly polymer coatings that minimize biofouling and protect steel from corrosion. Because siloxanes and fluorosilicones have been shown to be effective nontoxic foul release materials, siloxanes that contain pendant perfluoroalkyl groups have been prepared and the corrosion protection properties of films that were UV-cured with photoacid catalyst have been studied using electrochemical impedance spectroscopy (EIS).¹ Similar fluorinated siloxanes have also been converted to solid films by thermal cure with α, ω -diaminoalkanes.²

The corrosion behavior of the coated steel samples has been evaluated during exposure to 0.5 N NaCl as a function of exposure time using EIS, which, when properly applied, can be a nondestructive technique that allows monitoring of changes in the coating properties and corrosion rates of the substrate at locations where the coating has delaminated. The impedance spectra were analyzed using appropriate equivalent circuits (ECs).³⁻⁶ The resulting fit parameters can be related to the properties of the coating and the metal surface and their changes with exposure time to a corrosive solution.

Experimental

Two fluorinated pentasiloxanes [A, where $R_f = \text{CH}_2\text{CH}_2\text{CF}_3$, and B, where $R_f = \text{CH}_2\text{CH}_2(\text{CF}_2)_5\text{CF}_3$] and a nonfluorinated pentasiloxane (C, where $R = \text{CH}_3$) have been prepared as previously reported.^{1,2} Depending on the terminal epoxy group type, two different cross-linking/cure chemistries were utilized. The first type of crosslinking reaction involved room-temperature UV cure with a photoacid catalyst ("A", "B", "C").¹ The second cross-linking reaction was the phenol-catalyzed thermal cross-linking of A or C with α, ω -diaminoalkanes [$\text{NH}_2\text{-(CH}_2\text{)}_n\text{-NH}_2$, where $n = 6$ ("A6" or "C6"), 8 ("A8" or "C8"), or 12 ("A12" or "C12")].²

Coated steel coupons for corrosion testing were prepared as follows. A liquid epoxy-amine primer (3M Scotch-Weld EC-1945 B/A) was cast uniformly with a drawdown bar at 0.05 mm thickness onto

solvent-cleaned steel coupons [low-carbon, cold-rolled steel, $0.8 \times 76 \times 127$ mm with dull matte finish (P. N. Gardner Co.)]. The primer was allowed to dry for 24 h at room temperature and the sample was then placed in a 100°C oven for 1 h. The various liquid solutions were each coated over the primer layer at 0.13 mm thickness with a drawdown bar. Liquid layers of each A, B, and C and a photoacid catalyst (0.5 wt %) were UV-cured for 5 min. Liquid layers of each A6, A8, A12, C6, C8, and C12 and phenol catalyst (4 wt %) were cured overnight at 100°C.

Impedance spectra were obtained at -0.6 V because a stable E_{corr} could not be determined due to the high ohmic resistance of the coatings. The amplitude of the applied ac signal was 20 mV. The spectra have been recorded as a function of exposure time to 0.5 N NaCl in the frequency range of 100 KHz - 5 MHz. A saturated calomel electrode (SCE) and a type 316 stainless sheet were used as reference and counter electrode, respectively. The exposed area of the coated steel samples was 5 cm². A Gamry PCI4/300 potentiostat and Gamry EIS300 software were used for the impedance measurements. The spectra were analyzed using the COATFIT module of the ANALEIS software⁴ or the open boundary finite length diffusion (OFLD) model.⁵

Results and Discussion

Samples with UV-cured coatings A and B were exposed for 70 days and the sample with coating C was exposed for 35 days. Figure 1 shows the impedance spectra for these samples after 7, 21, and 35 days exposure. In the spectra for sample A the frequency dependence of the phase angle at the lowest frequencies indicates that the spectra agree with the OFLD model (Fig. 2) that describes processes in which diffusion occurs in a porous layer.⁵ In the EC in Fig. 2, C_c is the coating capacitance, R_p is the polarization resistance, and OFLD is the term that models the diffusion impedance that in Boukamp's notation is given by

$$Z_{\text{OFLD}} = [\tanh B(j\omega)^{1/2}] / Y_0(j\omega)^{1/2}$$

$$\text{where } B = d/(D)^{1/2} \quad \text{and} \quad Y_0 = [\sigma(2)^{1/2}]^{-1} \quad [1]$$

In Eq. 1 B is the diffusion parameter with diffusion length d and diffusion coefficient D and σ is the Warburg coefficient. For polymer coatings d is assumed to be equal to the coating thickness.

The impedance spectra for the fluorinated samples A and B and for the nonfluorinated sample C showed different changes with exposure time. The spectra for sample A agreed with the OFLD model and there was a significant decrease of the impedance values at low frequencies with time. The spectra for sample B agreed with the one-time-constant (OTC) model and showed only small changes

* Electrochemical Society Active Member.

** Electrochemical Society Fellow.

^z E-mail: mansfeld@usc.edu

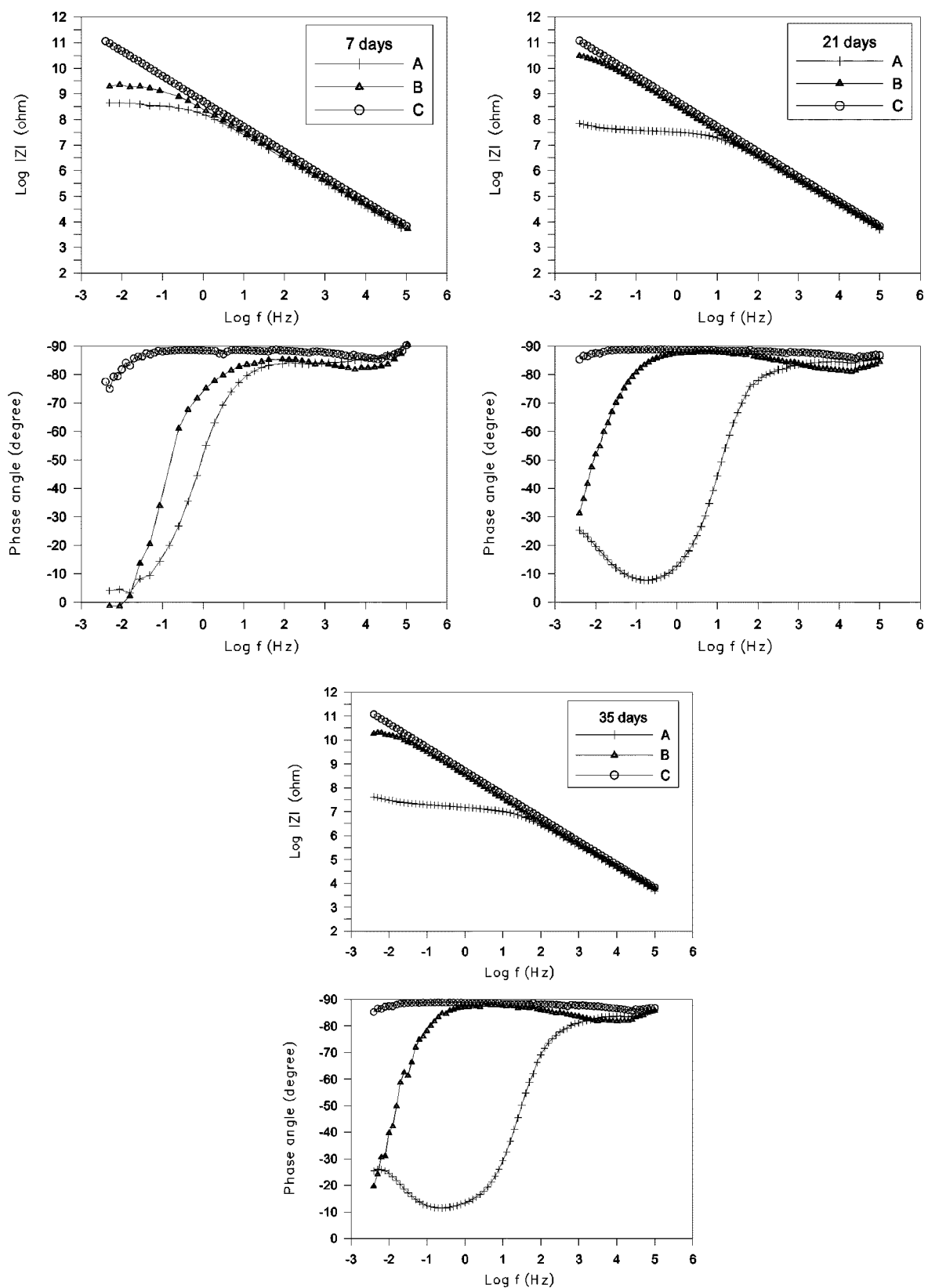


Figure 1. Impedance spectra of samples A, B, and C for 7, 21, and 35 days exposure to 0.5 N NaCl.

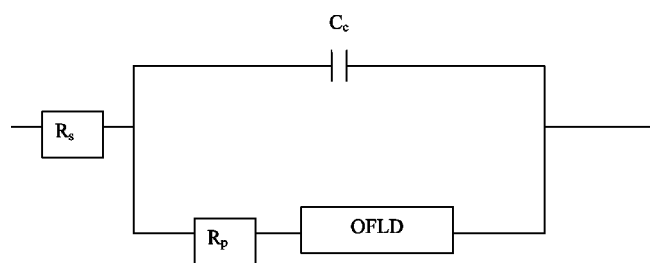


Figure 2. The OFLD model.

during exposure, which can be seen more clearly in the frequency dependence of the phase angle (Fig. 1). The spectra for sample C showed capacitive behavior and did not change much with time for 35 days. Figure 3 shows C_c and R_p as a function of time for samples A, B, and C. Initial cured dry thickness values of the coatings measured with a micrometer are also shown in Fig. 3. It can be seen that

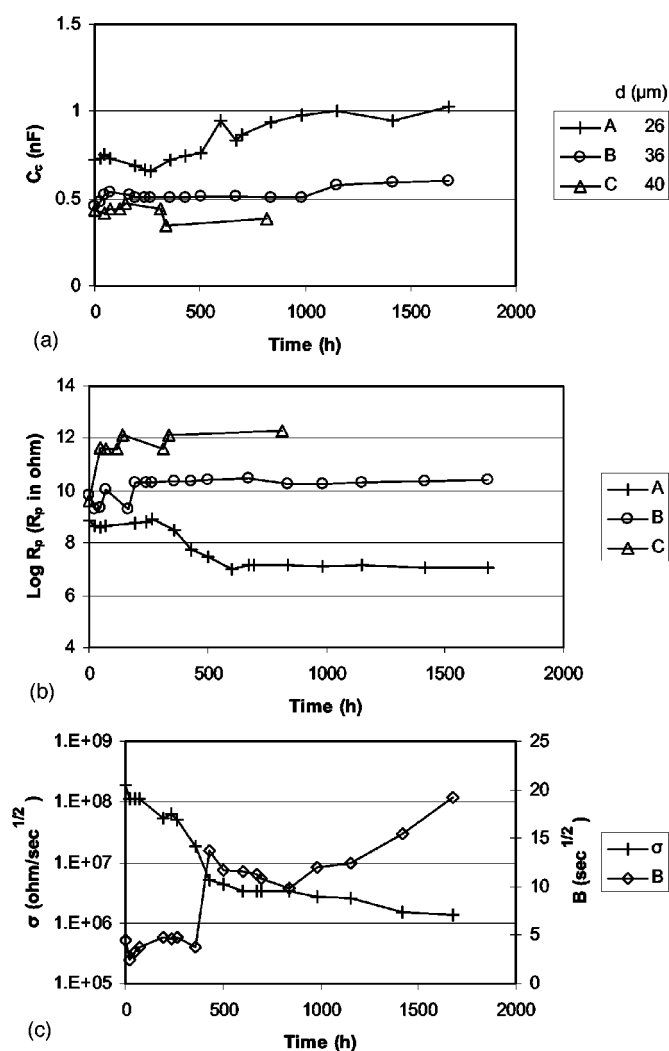


Figure 3. (a) Time dependence of C_c for coating types A, B, C; (b) time dependence of R_p for A, B, C; and (c) time dependence of Warburg coefficient σ and fit parameter B for A.

considerable shrinking of the coating had occurred during curing. Sample A, with the thinnest coating, had the highest values of C_c (Fig. 3a) and the lowest values of R_p (Fig. 3b). C_c increased with time while R_p decreased with time, indicating water uptake and coating degradation. Sample C, with the thickest coating, had the highest values of R_p . For sample B essentially no changes of C_c and R_p with time were observed. The Warburg coefficient σ for sample A decreased with time and the fit parameter B increased with time as the delaminated area increased⁵ (Fig. 3c). Based on the results shown in Fig. 3 it can be concluded that the coating C and to some extent also coating B provided excellent corrosion protection for steel exposed to 0.5 N NaCl.

Figures 4 and 5 show the impedance spectra for samples A, A6, A8, and A12 (Fig. 4), as well as C, C6, C8, and C12 (Fig. 5), for 7, 21, and 35 days of exposure to 0.5 N NaCl. The spectra for these samples agree with the coating model³⁻⁶ (Fig. 6) that describes the properties of the polymer coating layer and the corrosion reactions occurring on the steel surface at delaminated areas. C_c is shown in Fig. 7a as a function of time for samples A6, A8, A12, C6, C8, and C12. Samples A12 and C12 had the lowest initial C_c values because their coatings were thicker than the other coatings (Fig. 7a). The C_c values for these two coatings did not change much with exposure time. For samples A8, C6, and C8 C_c increased continuously with time, while for sample A6 C_c first increased and then decreased. R_{po} is the pore resistance due to the formation of ionically conducting paths in the coating. Its changes can be related with degradation of the coating as discussed below.³⁻⁶ Figure 7b shows the time dependence of R_{po} values for the same set of coatings. For samples A12 and C12 which had the highest R_{po} values, no significant changes of R_{po} as a function of time were observed. For samples A8, C6, and C8 a significant decrease in R_{po} values was found, while the decrease for sample A6 was not as pronounced. R_p is the polarization resistance of the delaminated area at the polymer/coating interface at which corrosion occurs, and C_{dl} is the corresponding capacitance. The time dependence of C_{dl} and R_p is shown in Fig. 7c and d, respectively. The changes of C_{dl} with time were quite small for all samples, except for sample A12 for which large fluctuations of C_{dl} were observed (Fig. 7c). For R_p at longer exposure times samples A8 and A12 had similar values which were lower than the R_p values for the other group of samples, including A6, C6, C8, and C12, which had very similar values at the end of the test.

The changes of C_{dl} , R_p , and R_{po} with exposure time can be related to the area of the steel surface at which corrosion occurs. The delamination ratio Δ can be defined as $\Delta = A_d/A_t$, where A_d is the delaminated area and A_t is the total exposed area.³⁻⁶ As coating porosity increases and A_d increases, R_p and R_{po} decrease while C_{dl} increases. R_{po} , R_p , and C_{dl} are related with A_d according to the following equations⁵

$$R_{po} = R_{po}^0/A_d$$

$$\text{with } R_{po}^0 = \rho d \text{ (ohm cm}^2\text{)} \quad [2]$$

$$R_p = R_p^0/A_d \quad [3]$$

$$C_{dl} = C_{dl}^0 A_d \quad [4]$$

$$C_c = (\epsilon \epsilon_0/d)(A_t - A_d) = C_c^0(A_t - A_d) \quad [5]$$

In Eq. 2, where ρ is the coating resistivity and d is the coating thickness, it has been assumed that ρ remains constant with exposure time. However, as shown below, ρ decreases with time to an extent that depends on coating formulation. Therefore Eq. 2 can be rewritten as

$$R_{po} = \rho d/A_t \Delta \quad [6]$$

It has been suggested that the extent of delamination can be determined qualitatively from the experimental values of the break-

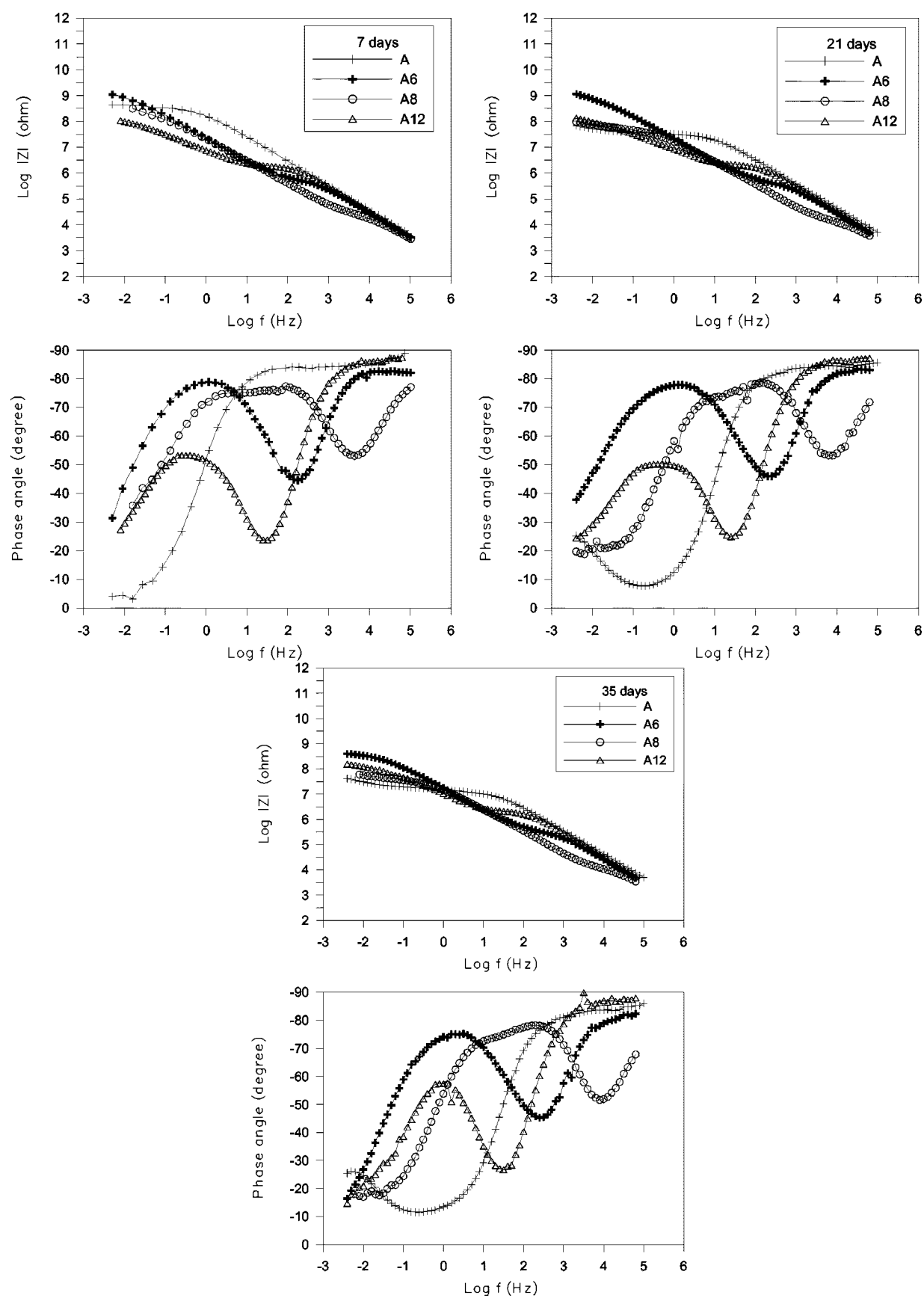


Figure 4. Impedance spectra of samples A, A6, A8, and A12, for 7, 21, and 35 days exposure to 0.5 N NaCl.

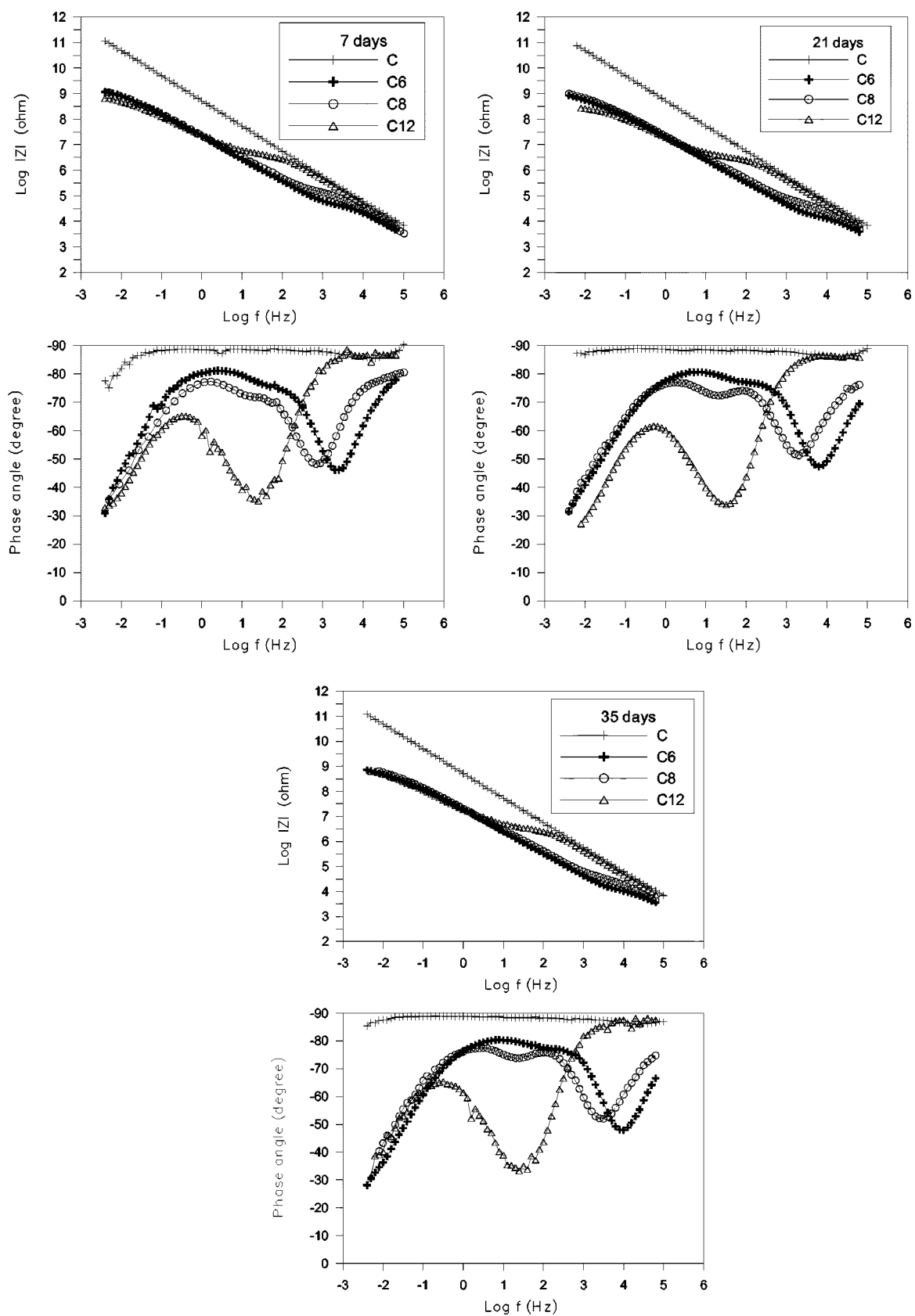


Figure 5. Impedance spectra of samples C, C6, C8, and C12 for 7, 21, and 35 days exposure to 0.5 N NaCl.

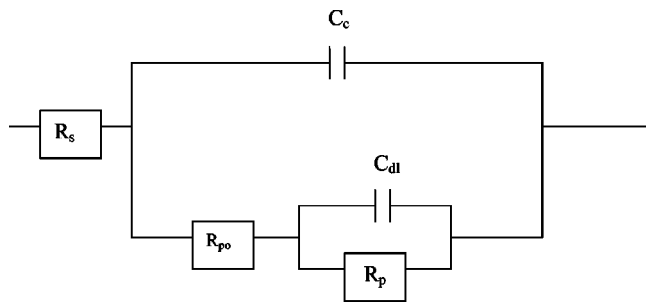


Figure 6. EC for coating model.

point frequency f_b , which is defined as the frequency at which the phase angle Φ equals -45° in the high-frequency region.^{3,7-9} The location of f_b is shown in Fig. 8a. The breakpoint frequency f_b is related to Δ and ρ according to the following relationships assuming $A_t \gg A_d$ ⁶

$$f_b = (2\pi R_{po} C_c)^{-1} = f_b^o A_d / A_t = f_b^o \Delta / \rho$$

$$\text{with } f_b^o = \frac{1}{2} \pi \epsilon \epsilon_0 \quad [7]$$

The f_b values for samples A and B are given in Fig. 9 as a function of exposure time. There is a significant difference between the f_b values of samples A and B during the whole exposure time. While for sample B f_b remained constant at very low frequencies, it increased continuously for sample A, indicating increased coating degradation. Figure 10a shows the time dependence of f_b for samples A12 and C12, which were the only two samples for which Φ had decreased below -45° at high frequencies. The breakpoint

frequencies for these two samples showed a similar initial increase but did not change much with time after about 200 h.

In addition to f_b , the minimum of the phase angle Φ_{\min} and its frequency f_{\min} can be used to qualitatively evaluate the delamination process of the coatings and to determine its Δ and ρ values.⁶ The Bode plot in Fig. 8a indicates the locations of Φ_{\min} and f_{\min} , which can be related to Δ and ρ as follows

$$f_{\min} = k_1 \Delta^{1/2} / \rho \quad \text{where } k_1 = (2\pi d)^{-1} (C_c^0 C_{dl}^0)^{-1/2} \quad [8]$$

$$\tan \Phi_{\min} = k_2 \Delta^{-1/2} \quad \text{where } k_2 = 2(C_c^0 / C_{dl}^0)^{1/2} \quad [9]$$

$$f_b / f_{\min} = k_3 \Delta^{1/2} \quad \text{where } k_3 = (C_{dl}^0 / C_c^0)^{1/2} \quad [10]$$

$$f_b / (f_{\min})^2 = k_4 \rho \quad \text{where } k_4 = 2\pi d C_{dl}^0 \quad [11]$$

The theoretical plots in Fig. 8b show that f_b and f_{\min} move to higher frequencies as coating degradation increases, while Φ_{\min} changes to less negative values. Figure 8c shows the dependence of f_b , f_{\min} , and Φ_{\min} on Δ .

Experimental values of Φ_{\min} and f_{\min} are shown as a function of time in Fig. 10b and c. For the more protective coatings A12 and C12 Φ_{\min} had values close to -30° , which did not change much with time, while for the other four samples it changed from about -40 to -50° for longer exposure times (Fig. 10b). For f_{\min} more or less constant values were found at low frequencies for A12 and C12, while for A6 f_{\min} had shifted to higher frequencies but did not change much with time. For the other three samples f_{\min} increased continuously with time (Fig. 10c). While the impedance spectra in Fig. 4 and 5 in general agree with model in Fig. 6, some inconsistencies are noted. For example, in Fig. 10b Φ_{\min} became more negative with exposure time for all samples except A12 and C12, which according to Eq. 9 and Fig. 8c implies that coating damage decreased with time for these samples, assuming that k_2 did not change with time. f_{\min} increased with time for samples A8, C6, and C8, suggesting that coating damage increased with time (Fig. 8c).

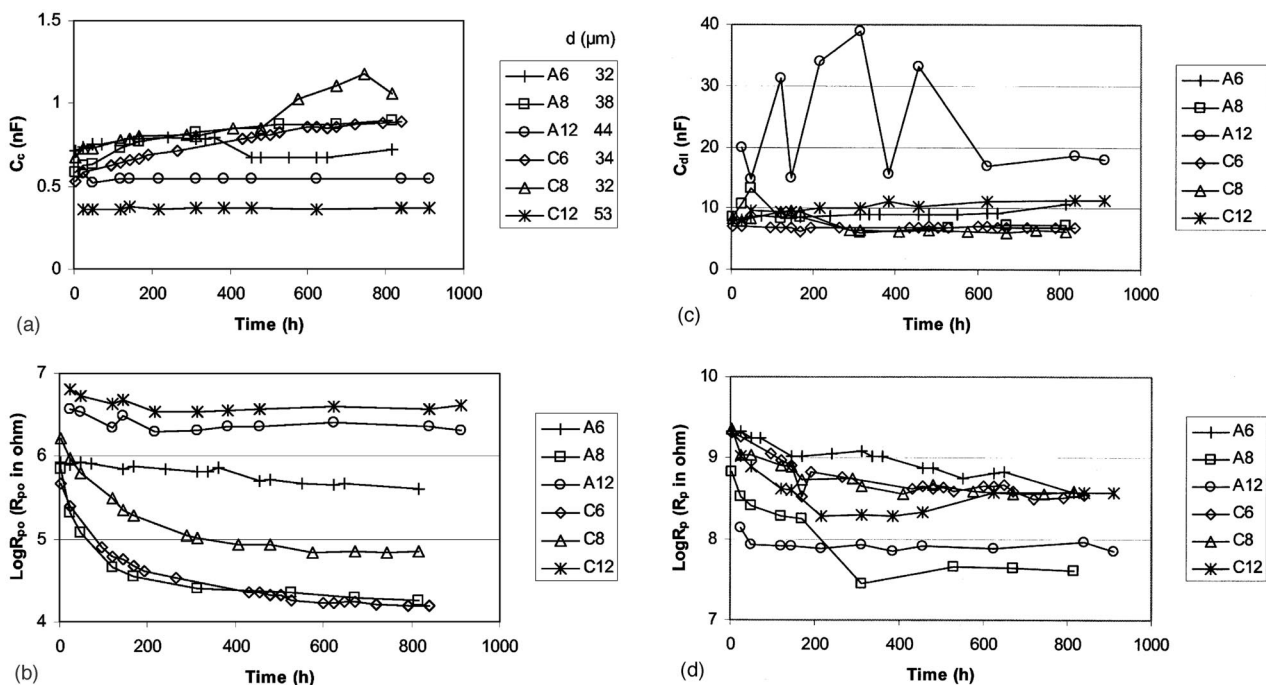


Figure 7. (a) Time dependence of C_c ; (b) time dependence of R_{po} ; (c) time dependence of C_{dl} ; and (d) time dependence of R_p .

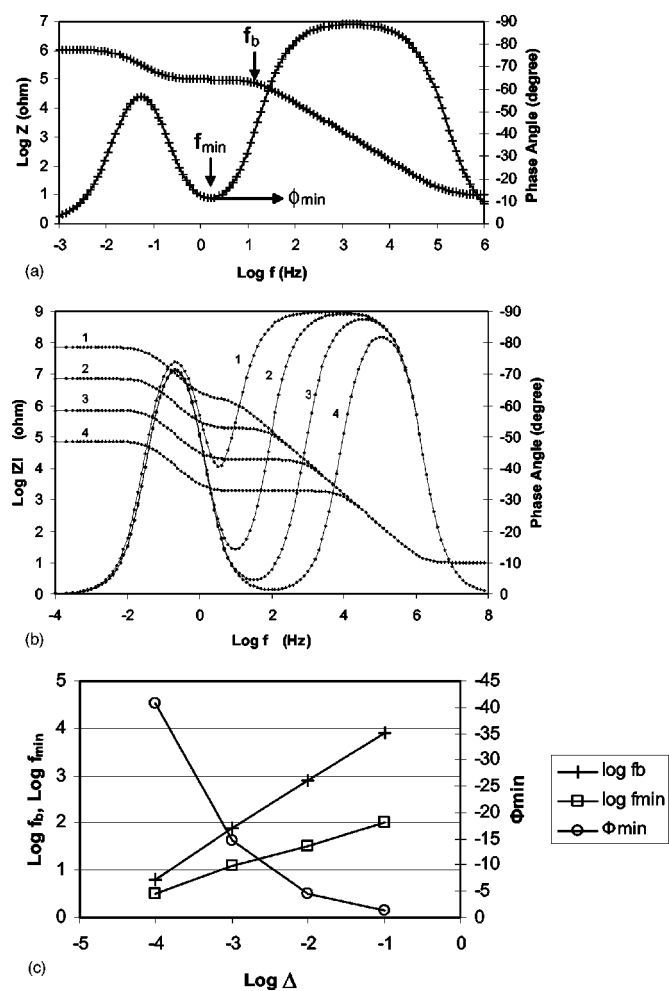


Figure 8. (a) Theoretical Bode plot according to the EC showing location of f_b , f_{min} , and Φ_{min} . (b) Theoretical impedance plots for a coating thickness of $d = 10 \mu\text{m}$ for different degrees of delamination: $\Delta = 10^{-4}$ (1), 10^{-3} (2), 10^{-2} (3), and 10^{-1} (4). (c) Dependence of f_b , f_{min} , and Φ_{min} on Δ .

The experimental values of Δ and ρ determined according to Eq. 9 and 8, respectively, are plotted as a function of time in Fig. 11a and b, respectively. For these calculations $C_{dl}^0 = 20 \mu\text{F}/\text{cm}^2$ was used and C_c^0 was taken as the C_c value for $t = 0$. The observed Δ -values in the range 0.002-0.005% for all samples except sample A12 (Fig. 11a) are very low and did not show significant changes with time, which suggests that defects that were present in the coating layers at the start of the exposure test did not become much

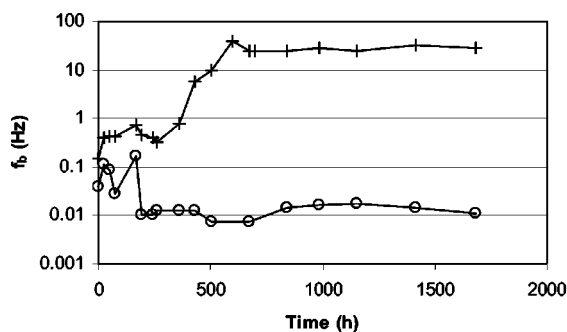


Figure 9. Time dependence of f_b for A and B.

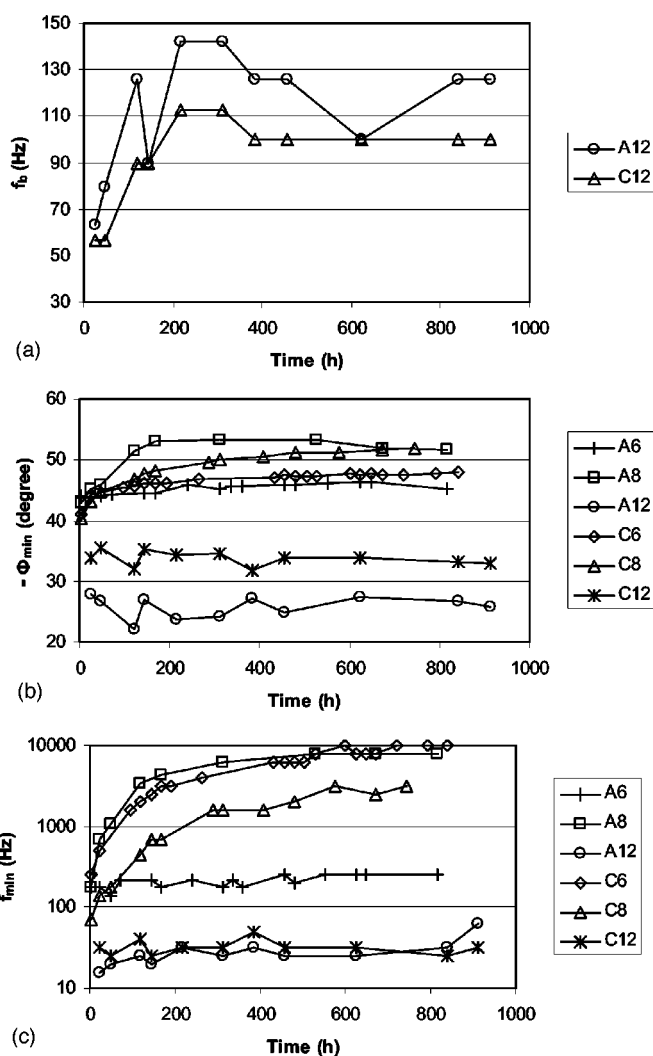


Figure 10. (a) Time dependence of f_b for A12 and C12; (b) time dependence of Φ_{min} for A6, A8, A12 and C6, C8, C12; and (c) time dependence of f_{min} for A6, A8, A12 and C6, C8, C12.

larger during exposure to 0.5 N NaCl. The almost constant high values of ρ between 100 and 1000 $\text{k}\Omega \text{cm}$ for samples A12 and C12 (Fig. 11b) are typical for polymer coatings and suggest that the coating layers remained more or less pore-free during exposure. For sample A6 ρ was lower by about a factor of ten but did not change much with time. For samples A8, C6, and C8, ρ decreased continuously to values close to 1 $\text{k}\Omega \text{cm}$ (Fig. 11b).

In order to check the validity of the coating model and the assumptions made in Eq. 2-11, theoretical values of R_{po} were calculated using Eq. 6 with the experimental values Δ (Fig. 11a) and ρ (Fig. 11b) and compared with the experimental values in Fig. 7b. Excellent agreement between these two groups of data was observed except for sample C12 at the highest values of R_{po} in the first 2 days of exposure (Fig. 12).

Conclusions

Sample C, which was a nonfluorinated pentasiloxane, provided the best corrosion protection among all coatings on the steel coupons evaluated here. Its impedance showed capacitive behavior at all frequencies and there were no significant changes of R_p and C_c

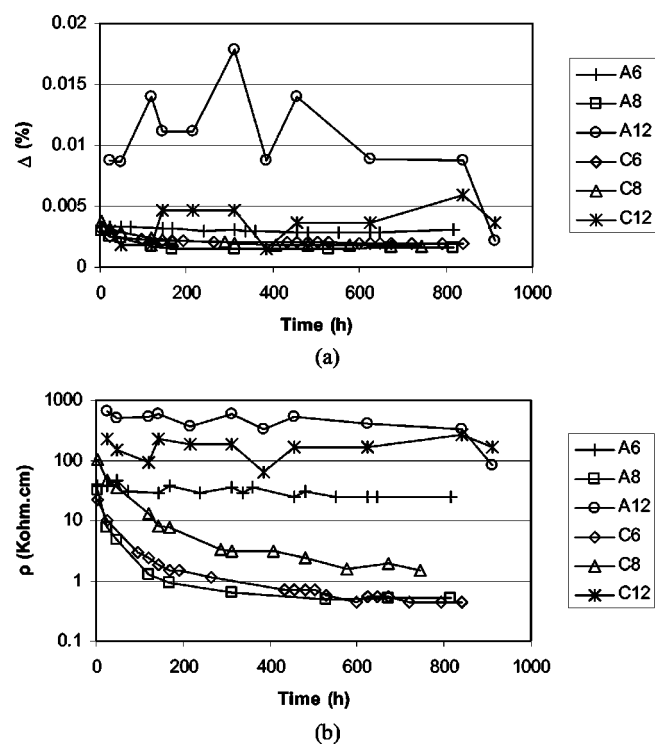


Figure 11. Time dependence of (a) the delamination ratio Δ and (b) specific coating resistivity ρ .

with at least 35 days exposure. The most significant changes in the coating properties were observed for sample A, which are assumed to be due to an increase of the delaminated area. The impedance spectra for samples with coatings prepared by phenol-catalyzed thermal cross-linking of A (fluorinated) and C (nonfluorinated) with α, ω -diaminoalkanes (6, 8, and 12) followed the coating model. The best corrosion protection was provided by coatings with cross-linkings of $n = 12$. The observation that fit parameters for samples A12 and C12 such as R_{po} , f_b , f_{min} , and Φ_{min} did not change significantly with time suggests that defects in the coatings that were present initially did not grow much with increasing exposure time.

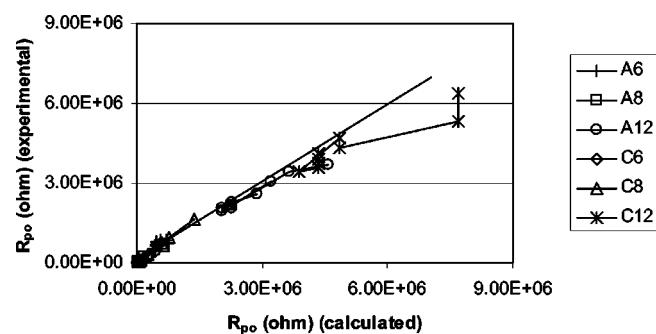


Figure 12. Comparison of calculated and experimental values of R_{po} .

The calculated coating resistivity was the highest for these two types of samples. The delamination ratio Δ was very small for all samples and did not change much with time. A somewhat surprising result is the finding that the calculated values of Δ were somewhat higher for A12 and C12 than for the other samples.

The results obtained in this study demonstrate that coating type and coating preparation can play an important role in corrosion protection of steel in corrosive media. The biofoul release properties of the coatings evaluated here are being investigated at present in a different task of this project.

Acknowledgment

This work was supported by the Office of Naval Research (N00014-02-1-0521).

The University of Southern California assisted in meeting the publication costs of this article.

References

1. M. A. Grunlan, N. S. Lee, G. Cai, T. Gaedda, J. M. Mabry, F. Mansfield, E. Kus, D. E. Wendt, G. L. Kowalke, J. A. Finlay, J. A. Callow, M. E. Callow, and W. P. Weber, *Chem. Mater.*, **16**, 2433 (2004).
2. M. A. Grunlan, N. S. Lee, and W. P. Weber, *J. Appl. Polym. Sci.*, **94**, 203 (2004).
3. F. Mansfield, *J. Appl. Electrochem.*, **25**, 187 (1995).
4. F. Mansfield, H. Shih, H. Greene, and C. H. Tsai, *ASTM Spec. Tech. Publ.*, **1188**, 37 (1993).
5. F. Mansfield, L. T. Han, C. C. Lee, and G. Zhang, *Electrochim. Acta*, **43**, 2933 (1998).
6. F. Mansfield and T. S. Tsai, *Corrosion (Houston)*, **47**, 958 (1991).
7. C. H. Tsai and F. Mansfield, *Corrosion (Houston)*, **49**, 726 (1993).
8. S. Haruyama, M. Asari, and T. Tsuru, in *Corrosion Protection by Organic Coatings*, M. Kendig and H. Leidheiser, Jr., Editors, PV 87-2, p. 197, The Electrochemical Society Proceedings Series, Pennington, NJ (1987).
9. R. Hirayama and S. Haruyama, *Corrosion (Houston)*, **47**, 952 (1991).